Thermoluminescence of natural $BeAl_2O_4:Cr^{3+}$ Brazilian mineral: preliminary studies

Neilo Marcos Trindade[1,2], Henrique Kahn[3], Elisabeth Mateus Yoshimura[2].

[1] Federal Institute of Education, Science and Technology of São Paulo - IFSP, Rua Pedro Vicente, 625, 01109010, São Paulo, SP, Brazil

e-mail: ntrindade@ifsp.edu.br; ORCID: 0000-0003-0202-907X

Telephone number: +18646338335

[2] University of São Paulo - USP, Institute of Physics, Rua do Matão, 1371, 05508090, São Paulo, SP, Brazil

e-mail: e.yoshimura@if.usp.br; ORCID: 0000-0003-4778-1230

[3] University of São Paulo - USP, Graduate Program in Mineral Engineering, Av. Prof. Mello Moraes, 2373, 05508900, São Paulo, SP, Brazil

email: henrkahn@usp.br; ORCID: 0000-0003-2437-4122

ABSTRACT

Alexandrite ($BeAl_2O_4:Cr^{3+}$) is a variety of the chrysoberyl mineral widely found in Brazil. This mineral is expected to have potential as a natural dosimeter since its composition contains 19.8 wt % BeO and 80.2 wt % Al_2O_3, both oxides being commercially used as dosimeters. We report the investigation of thermoluminescence (TL) properties from alexandrite in natural form. Samples 1.0 mm-thick and mass of 0.045 g were cut of a stone originated in Bahia, Brazil. Sample composition was determined through x-ray fluorescence and scanning electron microscopy/energy dispersive x-ray spectroscopy measurements. Irradiations were performed at room temperature using a $^{90}Sr/^{90}Y$ beta source of the Riso TL reader (dose rate = 10 mGy/s). TL measurements were made at 5ºC/s within the dose range from 1 to 50 Gy. The glow curve consists of a dominant peak at 350˚C and three additional peaks at 110, 160 and 280˚C. Results showed that the TL signal increases linearly with beta irradiation dose. Our results suggest that Fe and Cr ions together with the presence of secondary phases such as mica and apatite play important roles in the TL process. Based on the linearity of the TL response, we conclude that alexandrite shows potential for use in dosimetry.

Keywords: alexandrite, chrysoberyl, thermoluminescence, X-ray fluorescence, photoluminescence.

1. INTRODUCTION

Currently, Brazil is one of the largest producers of natural alexandrite mineral in the world. Nevertheless, despite belonging to families of gems of high economic and technological interest [1], there are few studies about the physical properties of natural alexandrite, for example, thermoluminescent properties.

Alexandrite, with chemical composition of $BeAl_2O_4:Cr^{3+}$, has a chrysoberyl type structure with the incorporation of chromium in its lattice [2]. The chrysoberyl ($BeAl_2O_4$) has the theoretical composition of 42.5 wt.% Al, 7.1 wt.% Be and 50.4 wt.% O, a chemical composition similar to that of spinel mineral group, and structurally isomorphic to olivine [3]. The chrysoberyl structure has orthorhombic symmetry (*Pmnb*) that corresponds to dense hexagonal packing, influencing oxygen atom (atomic radius 2.7 Å) positions, which are slightly distorted by the presence of aluminum atoms. The unit cell contains four molecules with eight Al^{3+} ions (0.54 Å) occupying distorted octahedral sites, and four Be^{2+} ions (0.47 Å) occupying distorted tetrahedral sites formed with oxygen ions located in planes perpendicular to the c-axis [4]. Due to the small ionic radius of Be^{2+}, the crystal structure of chrysoberyl has a lower symmetry than the spinel mineral group with similar chemical composition [5]; this small ionic radius also results in a bond length of 1.637 Å for Be-O [6]. Two of the three oxygen positions are located in a reflection plane and the third oxygen occupies a general position [7].

These distortions give rise to two sites of different symmetries: site, Al_1, average Al-O bond length of 1.890 Å, set in an inversion center symmetry and a site, Al_2, average Al-O length of 1.938 Å, located in a reflection plane [5,8,9]. In alexandrite, Cr^{3+} ions preferably occupy the largest of these sites, Al_2. Chromium impurities are responsible for the optical properties of this mineral, being used as laser emitter [4,6,10]. This mineral

also has a photochromatic effect that can be explained by the relative presence of chromium in both positions: Cr^{3+} (Al_2)/ Cr^{3+} (Al_1) [3]. This property, known in the literature as the alexandrite effect [11], results in the popularity and high market value of alexandrite as a gem [12]. Furthermore, the alexandrite crystal is mechanically rigid and has good thermal conductivity [12]. Alexandrite in synthetic form is also well known in the medical field as an active laser medium, first reported by Bukin et al. [13], with superior characteristics when compared to other types of laser media with emission in the range between 700 and 800 nm [9,14]. Comprehensive reports on the applications of the alexandrite laser in medicine can be found in [15-21].

This work presents results of thermoluminescence (TL) of natural samples of alexandrite mineral investigated under beta irradiation. TL is the light emitted under heating by insulating materials that were previously exposed to ionizing radiation. It is a thermally stimulated emission originating from the energy that was previously stored in the material during the irradiation [22]. Therefore, the material exposure to ionizing radiation generates charge carriers that populate trapping levels, with heating leading to the release of these carriers from the trapping centers [23]. The light emitted during heating is caused by the recombination of the released carriers with the opposite charge carriers in defects called recombination centers, where radioactive deexcitation occurs [24].

There are some naturally occurring minerals, such as quartz [25], topaz [26], feldspar [27] and mica [28] that present characteristics desired for TL dosimetry. However, in the literature, although there are many papers related to optical properties of alexandrite, to our knowledge, only one of them, by Yarovoi et al. [29], studied the

ionizing radiation effects in synthetic alexandrite and another paper, by Ferraz et al. [30], investigated the TL properties of natural alexandrite and chrysoberyl.

Yarovoi et al. [29] studied the creation of color centers in alexandrite irradiated by X rays and gamma rays and found out that the TL peak at 712 K (439°C) was related to these centers, with Cr^{3+} ions serving as the recombination centers. Ferraz et al. [30] showed TL measurements with the presence of the peaks at 170, 260 and 320°C, the latter being the most intense. The authors also claimed that chrysoberyl samples exhibits TL peaks at the same temperatures as in alexandrite samples, but with the glow curves being more than 200 times less intense.

In this work, the main motivation to investigate chrysoberyl is the fact that it contains 19.8 wt % BeO and 80.2 wt % Al_2O_3 [5]: both these crystals are commercially used as TL materials. BeO is used for ionizing radiation TL dosimetry, with high sensitivity, linear dose response and an effective atomic number (Zeff = 7.2) near to that of human soft tissue (Zeff ~7.6) [31]. Similarly, Al_2O_3 is a sensitive, well established material for luminescence dosimetry [32-34]. In both cases, studies are still in course to improve TL properties of these materials using different dopants [35,36]. For example, there are works with single crystals of Al_2O_3: Fe,Mg,Cr [37], and Al_2O_3:Cr,Ni [38]; additionally, recent works show Al_2O_3:C,Mg as a highly sensitive alternative luminescent material [39-41].

In this paper, we will present a series of experimental TL results of Brazilian alexandrite, relating the observations with the material impurities in order to explain the mechanism of the luminescence and the effects of ionizing radiation in this mineral.

2. MATERIALS AND METHODS

2.1 **Samples and preparation for analyses**

Our sample is a natural stone of alexandrite originated from Bahia, Brazil, with a dark green color. Two 1.0 mm-thick slices with mass of 0.045 g and perfectly parallel faces were cut from this stone, and denominated as *Ale I* and *Ale II*.

2.2 **Chemical analysis and photoluminescence**

Chemical analysis was carried out on polished sections of the samples by means of scanning electron microscopy (SEM)/electron dispersive X-ray spectroscopy (EDS) using Stereoscan 440 (LEO) with an energy dispersive spectrometer (EDS) (x-act, Oxford), imaged at accelerating voltage of 20 kV. For each section, back-scattered electron (BSE) imaging was used in complement to chemical characterization by EDS; EDS standardization was based on standards from Smithsonian Institute and Micro-Analysis Cons. Ltd. The characterization procedure also included standardless chemical analysis (total oxides) by nondestructive X-ray fluorescence (XRF) for major oxides (SiO_2, TiO_2, Al_2O_3, Fe_2O_3, MnO, MgO, CaO, Na_2O, K_2O, P_2O_5). The analyses were carried out using a Bruker S8 Tiger WD X-ray fluorescence spectrometer, with QuantExpress Full Analysis mode. The alexandrite samples were mounted in 40 mm diameter epoxy resin section blocks (Epofix–Struers) and then ground and polished with diamond for both SEM / EDS and XRF bulk analyses. Blank epoxy resin blocks were also analyzed to assure that there was no interference on analyses of the oxides.

Photoluminescence (PL) spectra were obtained using a Horiba Jobin Yvon Fluorolog 3 spectrofluorometer equipped with double monochromators for both excitation and detection, and a 450 W xenon lamp as the excitation source. All

144 measurements were carried out in ambient conditions and detection spectral resolution of
145 1 nm and integration time of 1s.
146
147 2.3 **TL measurements**
148 TL measurements were carried out using a commercial automated TL/OSL reader
149 produced by Risø National Laboratory (model DA-20). TL glow curves were obtained
150 using a heating rate of 5ºC/s, from room temperature to 450 ºC. The TL signals were
151 detected with a bialkali photomultiplier tube (PMT) behind an UV transmitting filter
152 (Hoya U-340, 7.5 mm thick). Irradiations were performed at room temperature using the
153 built-in $^{90}Sr/^{90}Y$ beta source of the TL/ OSL reader (dose rate of 10 mGy/s) at a dose
154 range from 1 to 50 Gy. Before use of a sample in a TL experiment, the sample was heated
155 at 20ºC/min up to 700 ºC and kept at this temperature for 1h, in a muffle furnace, to empty
156 the traps and erase any TL signal.
157
158 **3. RESULTS**
159 3.1 **Sample composition**
160 The emission and excitation spectra of the samples are shown in Figure 1. The
161 results agree with previously published results for both natural and synthetic alexandrite
162 samples [1,42], therefore, this outcome is consistent with the presence of Cr^{3+} in the
163 samples.
164 Table 1 shows the results of standardless XRF bulk concentration of major oxides
165 in both samples. Unfortunately, it is not possible to quantify beryllium with this
166 technique, as only elements with atomic numbers above B (Z=5) in the periodic table can
167 be detected, and only above F (Z=9) can be quantified with the QuantExpress mode.

Figure 2 presents BSE images of both samples, *Ale I* and *Ale II*. In these images, it is possible to identify other minerals in the samples, besides alexandrite, a fact that is common with natural samples. In order to identify these secondary phases some points were selected for ESD analysis based on the BSE images. In Tables 2 and 3 it is possible to see the results of EDS in these selected positions for both *Ale I* and *Ale II* samples.

3.2 **TL results**

Figure 3 shows the TL glow curves obtained for both samples at various irradiations doses (10 to 50 Gy). In the inset of the figure, the intensity of the high temperature peak as function of dose is presented. In addition, Figure 4 shows the linear regression from the normalized maximum values of the TL glow curves as a function of the dose. The parameters obtained by the linear fit are presented in Table 4. A study of the immediate fading of the TL signal was conducted, and Figure 5 shows the corresponding TL glow curves. In this experiment, the sample was beta irradiated and stored for some time (from 0 to 60 min) in the dark, at room temperature before the TL readout. In the inset of the figure we can observe the intensity of the main TL peak as function of time of storage.

4. DISCUSSION

In the case of alexandrite, two wide emission bands, and two lines (the R lines) are expected the spectrum. Figure 1 shows PL spectra of samples in different conditions of excitation/emission. The band centered at 570 nm corresponds to the overlapping of two emission bands of Cr^{3+} ions in two distinct sites Al_1 and Al_2 and the band centered at 420 nm, represents Cr^{3+} and Fe^{3+} also incorporated at different sites [42]. The broad bands are the strong vibrational of the $^4A_2$ to $^4T_2$ and $^4A_2$ to $^4T_1$ transitions, respectively [29,43]. R

192 lines, located between 680 and 678 nm at room temperature, not resolved in our
193 measurement, are associated with forbidden ^2E to $^4A_2$ transition of Cr^{3+} located at Al_2 sites
194 on a reflection plane [1,44,45]. This Cr^{3+} ions at Al_2 center are responsible for various
195 optical properties of alexandrite, for example, are responsible for the laser properties,
196 while the Cr^{3+} ions at Al_1 sites do not contribute to the luminescence spectra, or even
197 disfavor the process of ion excitation in the laser process [6,10,46].

198 It is possible to observe in Table 1 that, although both samples were extracted from
199 the same piece of rock, they present different levels of aluminum oxide, besides other
200 oxides. Sample *Ale II* contains a considerable amount of mineral impurities, including
201 CaO, SiO_2 and P_2O_5. Moreover, in sample *Ale II* the amount of Fe and Cr is about 45%
202 higher than in *Ale I* sample. Moreover, the presence of Fe in both the samples is
203 substantially large than Cr. The presence of Fe in alexandrite samples is important
204 because a high amount of this impurity may mask the identification of the optical
205 absorption bands attributed to Cr^{3+} in the host matrix [42].

206 In Figure 2, alexandrite mineral represents more than 98% of the *Ale I* sample and
207 75% of *Ale II*, which also contains 18% of phlogopite-biotite and 7% of apatite. Sample
208 *Ale I* is more homogeneous than sample *Ale II*, having compounds which are the basis of
209 alexandrite. However, when point measurements are taken in microfractures, the analysis
210 shows the presence of phlogopite-biotite with a higher SiO_2, MgO and Fe_2O_3 content. In
211 the sample *Ale I* there is a region composed of apatite with high a concentration of
212 phosphorus and calcium (light tone), another region with high a concentration of
213 aluminum, silicon, magnesium and iron (gray color, intermediate), and a third region
214 composed basically of alexandrite, also with the presence of phlogopite-biotite veins
215 (darker shade).

In Figure 3, both alexandrite samples show TL over a very wide temperature range with peaks at 110, 160 and 280 ˚C and a dominant peak at 350 ˚C. We can observe that *Ale II* sample emits about ten times more TL than sample *Ale I* for the same absorbed dose. The width and the shape of this peak suggest a superposition of several peaks. In the inset of Figure 3, we show the dose-response curves of the 350 ºC peak, that exhibits an almost linear growth with irradiation dose. In Figure 4, when we observe the normalized peak value obtained from the inset of Figure 3, the behavior of the points evidences a linear growth with the irradiation dose. In addition, in Table 4, we notice that, after normalization by the TL peak height for 50Gy, the linear behavior of both samples is the same, with similar slopes. As the TL peak positions are the same for both samples, and the quantities and varieties of impurities are diverse in the samples, we infer that the TL peaks are related to traps associated with intrinsic defects (related to the matrix atoms Al, Be, O) or to an impurity that is common for both samples. We speculate this also occurs with the sample studied by Ferraz et al. [30] as the peaks as very similar. Only the recombination centers might be of different nature in the various samples.

The TL intensity of sample *Ale II* may also be related to the mineral phases found. Barcena et al. [47] showed that the study of the TL of three different types of micas, muscovites, sericite and phologopites, from Spain, exhibit the presence of different and complex glow peaks. The mica has glow peaks in a temperature range of 160 to 400 °C. In particular, beta irradiation of muscovite samples was found to induce complex glow peak between 150 and 170 °C with a large high temperature signal, similar to our results in this work. Kalita and Wary [28] also observed the TL peak around 70 °C in a muscovite from India and mention that muscovite and biotite commonly coexist with quartz and

239 feldspar, which are widely used as natural dosimeters for luminescence dating and
240 retrospective dosimetry [48,49].

241 In addition, according to Barcena et al. [47] the emissions obtained for the micas
242 are related to Mn^{2+} ions in octahedral coordination, but more research is needed to know
243 if this peak is or not related to other cations or different defects in their lattice. Besides
244 the presence of micas, the sample *Ale II* contains a considerable presence of apatite.
245 According to Roman-Lopez et al. [50], that studied the luminescence of natural apatite in
246 Brazil, the samples present TL peak at 370 °C.

247 Yoshimura [37] investigated the TL emission in aluminum oxide single crystal
248 doped with Cr, Mg and Fe and the results show a TL glow curve with four peaks (110,
249 160, 225 and 270˚C). The trapping center responsible for the 160 ˚C peak was related to
250 intrinsic defects, and that the other TL glow peak positions are impurity dependent.
251 Mittani et al. [51] also observed a peak at 165 ˚C in all the glow curves with different
252 doses for natural beryl exposed gamma irradiation. Those authors suggested that this
253 process involves Fe^{3+} ions.

254 Ferraz et al. [30], also correlates a presence of Fe^{3+} with TL emission, however, at
255 320˚C. The authors suggested that the pre-annealing at temperatures higher than 600 ˚C
256 (in our case 700 ºC for 1h), in alexandrite, induces the $Fe^{2+} \rightarrow Fe^{3+}$ conversion in natural
257 sample and that an increase in the Fe^{3+} ion content improves TL emission. This is because
258 these ions can capture electrons during irradiation, playing a role of electron traps.
259 Pokorny and Ibarra [52] reported that the presence of the peak at 330˚C in Cr doped Al_2O_3
260 samples is related to the presence of Cr^{4+} ions. They concluded that the peak is related to
261 the F centers and their recombination with Cr^{4+} ions. Lapraz et al. [53] commented about
262 a similar peak, which is attributed by them to a conversion of the Cr^{2+} (or Cr^{4+}) centers to

Cr^{3+}. As in our samples it is also possible to notice (Figure 3) a peak around 275 to 295 ˚C, we might associate it with the same origin.

It is possible to observe in Figure 5 that, for both samples, the first peak, at 110 ˚C, is unstable at room temperature. When the time interval between the sample irradiation and the TL measurement increases, the peak diminishes and moves towards higher temperatures, extinguishing the TL band in 1h. The temperature shift may indicate the influence of the 160 ˚C peak, which does not fade, but can also point to the presence of a continuous distribution of activation energies for the corresponding trap. Except for this peak (110 ˚C), we observe qualitatively that the area remains constant because the other peaks do not have significant changes in the intensity with the storage time in the dark, and the TL glow curves continue with the same characteristics discussed before. In inset of the Figure 5, *Ale I* sample had a reduction of 6% in the intensity of the high temperature peak in relation to its initial value with 1h in the dark, while sample *Ale II* showed a reduction of 3%. Therefore, the samples are stable at room temperature up to 1 hour after the exposure to radiation, an important characteristic for dosimetry.

5. CONCLUSIONS

In this study we worked with two samples from the same mineral rock. The SEM / EDS results show that both samples have microfractures filled by micaceous minerals; but sample *Ale II* also presents a larger content of mica and apatite when compared to sample *Ale I*. Results like this may somehow be expected in natural materials, as the environment, the temperature and other important parameters of the mineral forming process might influence the incorporation of elements in different parts of the rock. The TL glow curve consists three peaks at 110, 160 and 280 ˚C and a dominant peak at 350

˚C. Comparing the samples, in the XRF, the sample *Ale II* presents higher content of silicon, calcium and phosphorus in relation to the sample *Ale I*, but by the EDS we conclude that these elements are present in the minor phase minerals. As the TL glow curves of both samples are very similar, regardless the presence of other mineral phases, it can be concluded that in the results of TL, the more prominent intensity in the *Ale II* sample may be related to the other observed mineral impurities: for instance, this can be related to the amounts of Cr and Fe that are higher for sample *Ale II* than for *Ale I*.

It was possible to observe that alexandrite shows potential for use in TL dosimetry. TL signal increased linearly with dose using beta excitation. Both samples, despite their individual peculiarities, presented a decrease of less than 10% in the intensity of the main peak in the reading after 1h in the dark. In addition, when linear regression of dose intensity values was performed, both samples had the same angular coefficient of 0.0199. Our investigation strongly supports the position that Fe and Cr ions interfere in the obtained results, generating TL broad bands that suggest the superposition of several peaks. A more detailed characterization of a larger number of samples and different regions of Brazil is being investigated. A deconvolution analysis of the TL curve should be done in later studies to better study on each of the TL peaks and to analyze the structure of the trap of this material, subsequently, the activation energy values can be estimated.

6. ACKNOWLEDGMENTS

Funding for this work was provided by Brazilian agencies São Paulo Research Foundation (FAPESP), grant #2010/16437-0 and #2016/22984-0, and National Council for Scientific and Technological Development (CNPq). The authors are grateful to Dr. Luiz G. Jacobsohn (Department of Materials Science and Engineering, Clemson

University, USA) for the use of the spectrofluorometer and discussion of the results.

7. REFERENCES

[1] N. Ollier, Y. Fuchs, C. Olivier, A.H. Horn, S. Rossano, Influence of impurities on Cr^{3+} luminescence properties in Brazilian esmerald and alexandrite. European Journal of Mineralogy **27** (2015) 783-792. doi: 10.1127/ejm/2015/0027-2484.

[2] M. Rossi, M. Dell´Aglio, A. Giacomo, R. Gaudiuso, G.S. Senesi, O. Pascale, F. Capitelli, F. Nestola, M.R. Ghiara, Multi-methodological investigation of kunzite, hiddenite, alexandrite, elbaite and topaz, based on laser-induced breakdown spectroscopy and conventional analytical techniques for supporting mineralogical characterization. Physics and Chemistry of Minerals **41** (2014) 127–140. doi: 10.1007/s00269-013-0631-3.

[3] K.J. Petersen Jr, Alexandrita no municipio de Minaçu, Goiás: Mineralogia, Geologia e considerações genéticas (Portuguese), Dissertation, USP, São Paulo, 1998.

[4] R.M.F. Scalvi, L.O. Ruggiero, M. Siu Li, Influence of annealing on X-ray diffraction of natural alexandrite. Powder Diffraction **17** (2002) 135-138. doi: 10.1154/1.1428284.

[5] V.Y. Ivanov, V.A. Pustovarov, E.S. Shlygin, A.V. Korotaev, A.V. Kruzhalov, Electronic excitations in $BeAl_2O_4$, Be_2SiO_4, and $Be_3Al_2Si_6O_{18}$ crystals. Physics of the Solid State, **47** (2005), 466 – 473. doi: 10.1134/1.1884706.

[6] S.U. Weber, M. Grodzicki, W. Lottermoser, G.J. Redhammer, G. Tippelt, J. Ponahlo, G. Amthauer, ^{57}Fe Mossbauer spectroscopy, X-ray single-crystal diffractometry, and electronic structure calculations on natural alexandrite. Physics and Chemistry of Minerals **34** (2007) 507-515. doi: 10.1007/s00269-007-0166-6.

335 [7] P. Bauerhansl, A. Beran, Trace hydrogen in the olivine-type minerals chrysoberyl,
336 Al_2BeO_4 and sinhalite, $MgAlBO_4$ – A polarized FTIR spectroscopic study.
337 Schweizerische Mineralogische und Petrographische Mitteilungen **77** (1997) 131 –
338 136.
339 [8] M.K. Rabadanov, A.P. Dudka, Comparative structural study of Al_2BeO_4 and
340 $Al_2BeO_4:Cr^{3+}$. Inorganic Materials **33** (1997) 48 – 51.
341 [9] R.M.F. Scalvi, M. Siu Li, L.V.A. Scalvi, Thermal annealing-induced electric dipole
342 relaxation in natural alexandrite. Physical and Chemistry of Minerals **31** (2005)
343 733-737. doi: 10.1007/s00269-004-0442-7.
344 [10] D.A. Vinnik, D.A. Zherebtsov, S.A. Archugov, M. Bischoff, R. Niewa, Crystal
345 growth and characterization of Alexandrite. Crystal Grow & Design **12** (2012)
346 3954-3956. doi: 10.1021/cg300344g.
347 [11] E. Gubelin, Alexandrite from Lake Manyara, Tanzania. Gems & Gemology **15**
348 (1976) 203-209.
349 [12] S.C. Collins, T.D. Wilkerson, V.B. Wilckwar, D. Rees, J.C. Walling, D.F. Heller,
350 The alexandrite ring laser: A spectrally narrow lidar light source for atmospheric
351 fluorescence and absorption observations. Advances in Atmospheric Remote
352 Sensing with Lidar. Berlin: Springer Verlag (1997) 577-580. doi: 10.1007/978-3-
353 642-60612-0_140.
354 [13] G.V. Bukin, S.Y. Volkov, V.N. Matrosov, Optical generation in alexandrite
355 ($BeAl_2O_4:Cr^{3+}$). Kvant Tovaya Electronika **5** (1978) 1168 – 1169.
356 [14] L.A.R.Torezan, N. Osório, Laser em Dermatologia: princípios físicos, tipos e
357 indicações. Brazilian Annals of Dermatology **74** (1990) 13 – 20.

[15] S. Toosi, A.H. Ehsani, P. Noormohammadpoor, N. Esmaili, M. Mirshams-Shahshahani, F. Moineddin, Comparation between Sequentional Treatment with Diode and Alexandrite Lasers versus Alexandrite Laser Alone in the Treatment of Hirsutism, Journal of the European Academy of Dermatology and Venereology **24** (2010) 470-473. doi: 10.1111/j.1468-3083.2009.03448.x.

[16] O.A. Ibrahimi, M.M. Avram, C.W. Hankes, S.L. Kilmer, R.R. Anderson, Laser hair removal. Dermatologic Therapy **24** (2011) 94-107. doi: 10.1111/j.1529-8019.2010.01382.x.

[17] M.A. Nilforoushzadeh, F.F. Naieni, A.H. Siadat, L. Rad, Comparation between sequentional treatment with diode and alexandrite lasers versus alexandrite laser alone in the treatment of hirsutism. Journal of Drugs in Dermatology **10** (2011) 1255-1259.

[18] Y. Li, X. Tong, J. Yang, L. Yang, J. Tao, Y. Tu, Q-switched alexandrite laser treatment of facial and labial lentigines associated with Peutz-Jeghers syndrome. Photodermatology, Photoimmunology & Photomedicine **28** (2012) 196-199. doi: 10.1111/j.1600-0781.2012.00672.x.

[19] N. Saedi, A. Metelitsa, K. Petrell, K.A. Arndt, J.S. Dover, Treatment of tattoos with a picosecond alexandrite laser. Arch Dermalogy **148** (2012) 1360-1363. doi: 10.1001/archdermatol.2012.2894.

[20] Y. Wang, H. Qian, Z. Lu, Treatment of café au lait macules in Chinese patients with a Q-switched 755-nm alexandrite laser. Journal of Dermatological Treatment **23** (2012) 431-436. doi: 10.3109/09546634.2011.590790.

[21] Y.K. Kim, D.Y. Kim, S.J. Lee, W.S. Chung, S.B. Cho, Therapeutic efficacy of long-pulsed 755-nm alexandrite laser for seborrheic keratoses. Journal of the European

Academy of Dermatology and Venereology **28** (2014) 1007-1011. doi: 10.1111/jdv.12231.

[22] E.G. Yukihara, Desvendando a Cor e Termoluminescência do Topázio: Um Estudo dos Defeitos e Processos Termicamente e Opticamente Estimulados no Cristal Natural (Portuguese). Thesis, USP, São Paulo, 2001.

[23] L.G. Jacobsohn, A.L. Roy, C.L. Mcpherson, C.J. Kucera, L.C. Oliveira, E.G. Yukihara, J. Ballato, Rare earth-doped nanocrystalline MgF_2: Synthesis, luminescence and thermoluminescence. Optical Materials **35** (2013) 2461-2464.

[24] S.W.S. Mckeever, Thermoluminescence of Solids, Cambridge, England, Cambridge University Press, 1985.

[25] I.K. Bailiff, L. Bøtter-Jensen, V. Correcher, A. Delgado, H.Y. Goksu, H. Jungner, S.A. Petrov, Absorbed dose evaluations in retrospective dosimetry: methodological developments using quartz. Radiation Measurements **32**(5-6). (2000) 609-613. doi: 10.1016/S1350-4487(00)00076-7.

[26] D.N. Souza, M.E.G. Valerio, J.F. de Lima, L.V.E. Caldas, Dosimetric properties of natural Brazilian topaz: A thermally stimulated exoeletronic emission and thermoluminescence study. Nuclear Instruments & Methods In Physics Research Section B-Beam Interactions With Materials and Atoms **166**(2000) 209-214. doi: 10.1016/S0168-583X(99)00746-6.

[27] V. Correcher, J.M. Gomez-Ros, J. Garcia-Guinea, Radiation effect on the 400nm-thermoluminescence emission of a potassium rich feldspar. Radiation Measurements **38**(4-6) (2004) 689-693. doi: 10.1016/j.radmeas.2003.12.006.

[28] J.M. Kalita, G. Wary Dosimetric characteristics of muscovite mineral studied under different annealing conditions. Physica Scripta **90** (2015) 055702. doi:10.1088/0031-8949/90/5/05570.

[29] P.N. Yarovoi, V.Y. Medvedev, G.V. Bukin, L.A. Ivanova, A.A. Mikhalenko, Radiative Creation of Color Centers in Alexandrite Crystals. Opt. Spectrosc. (USSR) **71(5)** (1991) 447–449.

[30] G.M. Ferraz, S. Watanabe, S.O. Souza, R.M.F. Scalvi, TL, EPR and Optical Absorption studies on natural alexandrite compared to natural chrysoberyl. Radiation Protection Dosimetry **100** (2002) 471-474.

[31] D.P. Groppo, L.V.E. Caldas, Luminescent response from BeO exposed to alpha, beta and X radiations. Radiation Measurements **71** (2014) 81-85. doi: 10.1016/j.radmeas.2014.07.009.

[32] E.G. Yukihara, S.W.S. Mckeever, Optically Stimulated Luminescence: Fundamentals and Applications. West Sussex, UK: John Wiley and Sons, Ltd., 2011.

[33] A.N. Nyerenda, M.L. Chitambo, The influence of radiation-induced defects on thermoluminescence and optically stimulated luminescence of α- Al_2O_3:C. Nuclear Instruments and Methods in Physics Research B **397** (2017) 92-100. doi: 10.1016/j.nimb.2017.02.077.

[34] V. Kortov, I. Milman, Some new data on thermoluminescence properties of dosimetric α- Al_2O_3:C crystals. Radiation Protection Dosimetry **65** (1996) 179-184. doi:10.1093/oxfordjournals.rpd.a031616.

[35] N. Salah, Z.H. Khan, S.S. Habib, Nanoparticles of Al_2O_3: Cr as a sensitive thermoluminescent material for high exposures of gamma rays irradiations. Nuclear

Instruments and Methods in Physics Research B **269** (2011) 401-404. doi: 10.1016/j.nimb.2010.12.054.

[36] Q. Liu, Q.H. Yang, G.G. Zhao, S.Z. Lu, H.J. Zhang, The thermoluminescence and optically stimulated luminescence properties of Cr-doped alpha alumina transparent ceramics. Journal of Alloys and Compounds **579** (2013) 259-262. doi: 10.1016/j.jallcom.2013.06.070.

[37] E.M. Yoshimura, Correlation of optically stimulated luminescence and thermoluminescence of Al_2O_3: Fe, Mg, Cr crystals. Nuclear Instruments and Methods in Physics Research A **580** (2007) 606-609. doi: 10.1016/j.nima.2007.05.021.

[38] P. Pokorny, A. Ibarra, On the origin of the thermoluminescence of Al_2O_3: Cr, Ni. Journal of Physics: Condensed Matter **5** (1993) 7387-7396.

[39] J.M. Kalita, M.L. Chitambo, On the sensivity of thermally and optically stimulated luminescence of α- Al_2O_3:C and α- Al_2O_3:C,Mg. Radiation Measurements **99** (2017) 18-24.

[40] J.M. Kalita, M.L. Chitambo, Comprehensive kinetic analysis of thermoluminescence peaks of α- Al_2O_3:C,Mg. Journal of Luminescence **185** (2017) 72-82.

[41] J.M. Kalita, M.L. Chitambo. Thermoluminescence of α- Al_2O_3:C,Mg: kinetic anyalysis of the main glow peak. Journal of Luminescence **182** (2017) 177-182.

[42] N.M. Trindade, R.M.F. Scalvi, L.V.A. Scalvi, Cr^{3+} distribuiton in Al_1 and Al_2 sites of alexandrite ($BeAl_2O_4$:Cr^{3+}) induced by annealing, investigated by optical spectroscopy. Energy and Power Engineering **2010** (2010) 18-24. doi: 10.4236/epe.2010.21004.

[43] J. C. Walling, O. G. Peterson, H. P. Jenssen, R. C. Morris, E. W. O'Dell, Tunable Alexandrite Lasers. IEEE Journal of Quantum Electronics **QE-16** (1990) 1302 – 1315.

[44] R.C. Powell, L. Xi, X. Gang, G.J. Quarles, J.C. Walling, Spectroscopy properties of alexandrite crystals. Physical Review B **32** (1985) 2788 – 2797.

[45] A.B. Suchocki, G.D. Gilliland, R.C. Powell, J.M. Bowen, J.C. Walling, Spectroscopy properties of alexandrite crystals II. Journal of Luminescence **37** (1987) 29-37. doi: 0.1016/0022-2313(87)90179-7.

[46] B.K. Sevest'yanov, Excited-State Absorption Spectroscopy of Crystals Doped with Cr^{3+}, Ti^{3+}, and Nd^{3+} Ions - Review. Crystallography Reports **48** (2003) 989 -1011. doi: 10.1134/1.1627442.

[47] J.L. Barcena, M. Urbina, A.P. Rowlands, P. Beneitez, A. Millan, T. Calderon, Basic thermoluminescence properties of micas: muscovite, sericite and phlogopite. Radiation Protection Dosimetry **84** (1999) 289-292.

[48] H.Y. Goksu, P. Schwenk. Thermoluminescence dating of terrazzo from the monastery church of Tegernsee (Bavaria, Germany) using the 210 degrees C TL peak of quartz. Radiation And Environmental Biophysics **39**(4) (2000) 301-308. doi: 10.1007/s004110000063

[49] V. Correcher, J.M. Gomez-Ros, A. Delgado. The use of albite as a dosimeter in accident dose reconstruction. Radiation Protection Dosimetry **84**(1-4) (1999) 547-549. doi: 10.1093/oxfordjournals.rpd.a032795.

[50] J. Roman-Lopez, V. Correcher, J. Garcia-Guinea, P. Prado-Herrero, T. Rivera, I.B. Lozano, Effect of the chemical impurities on the luminescence emission of natural

apatites. Spectrochimica Acta Part A: Molecular and Biomolecular Spectroscopy **126** (2014) 142-147. doi: 10.1016/j.ssa.2014.01.128.

[51] J.C.R. Mittani, S. Watanabe, J.F.D. Chubaci, M. Matsuoka, D.L. Baptista, F.C. Zawislak, Nuclear Instruments and Methods in Physics Research B **191** (2002) 281-284.

[52] P. Pokorny, A. Ibarra, Impurity effects on the thermoluminescence of Al_2O_3. Journal of Applied Physics **75 (2)** (1994) 1088-1092

[53] D. Lapraz, P. Iacconi, D. Daviller, B. Guilhot, Thermostimulated luminescence and fluorescence of α-Al_2O_3: Cr^{3+} samples (ruby). Physica Status Solidi (a) **126** (1991) 521-531.

FIGURE CAPTIONS

Figure 1 Excitation and emission spectra of *Ale I* and *Ale II* samples of natural alexandrite.

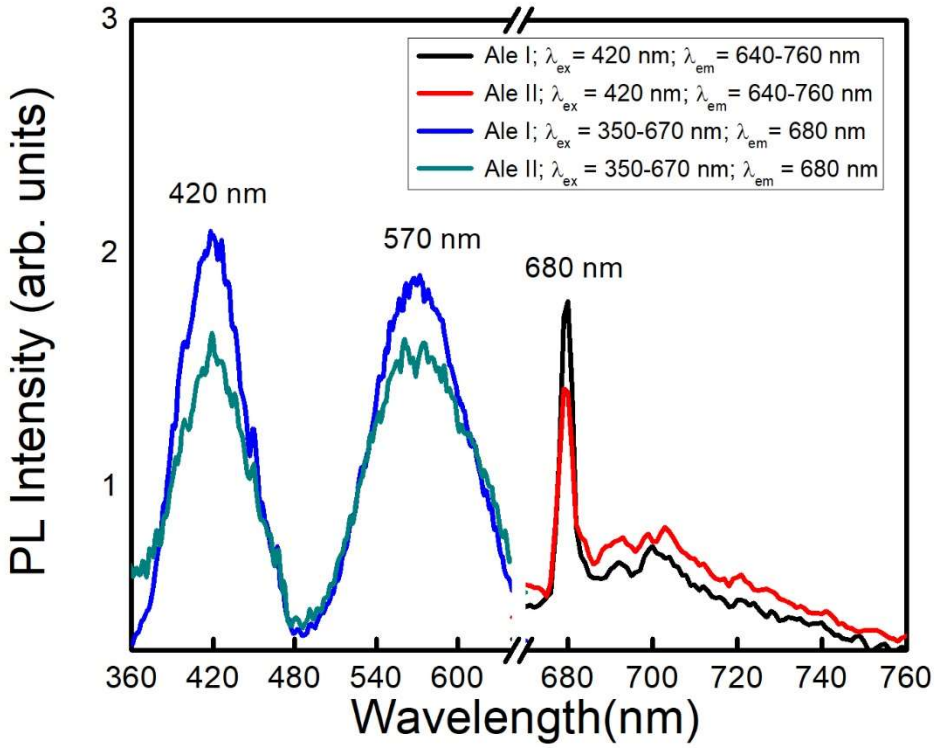

498 **Figure 2** BSE images of *Ale I* (a) and *Ale II* (b) alexandrite samples with minor phases

499 associated; Al – alexandrite; M – mica (phlogopite-biotite) and Ap - apatite.

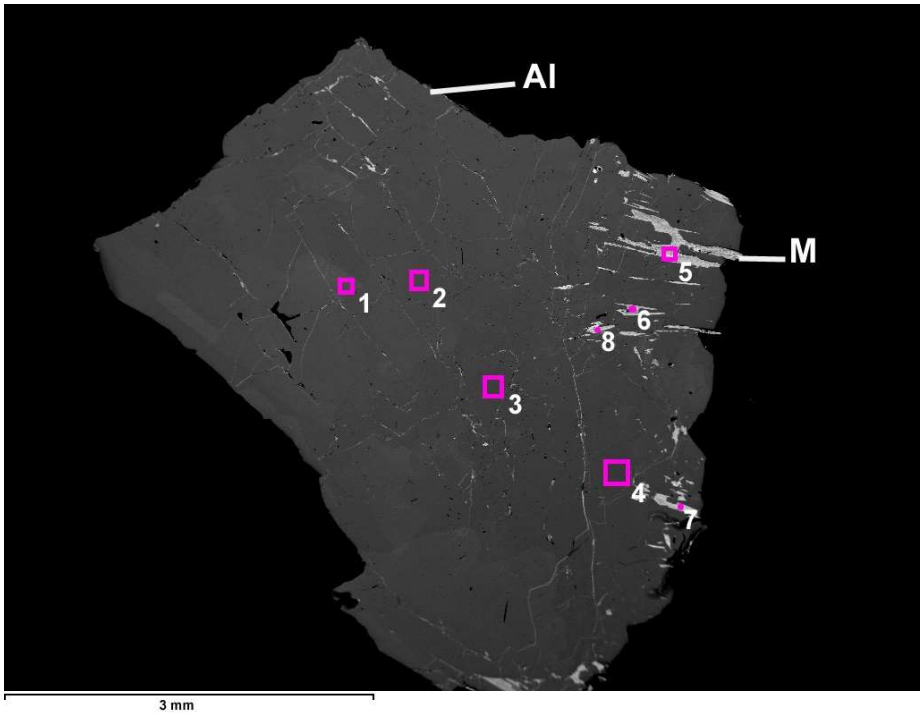

500

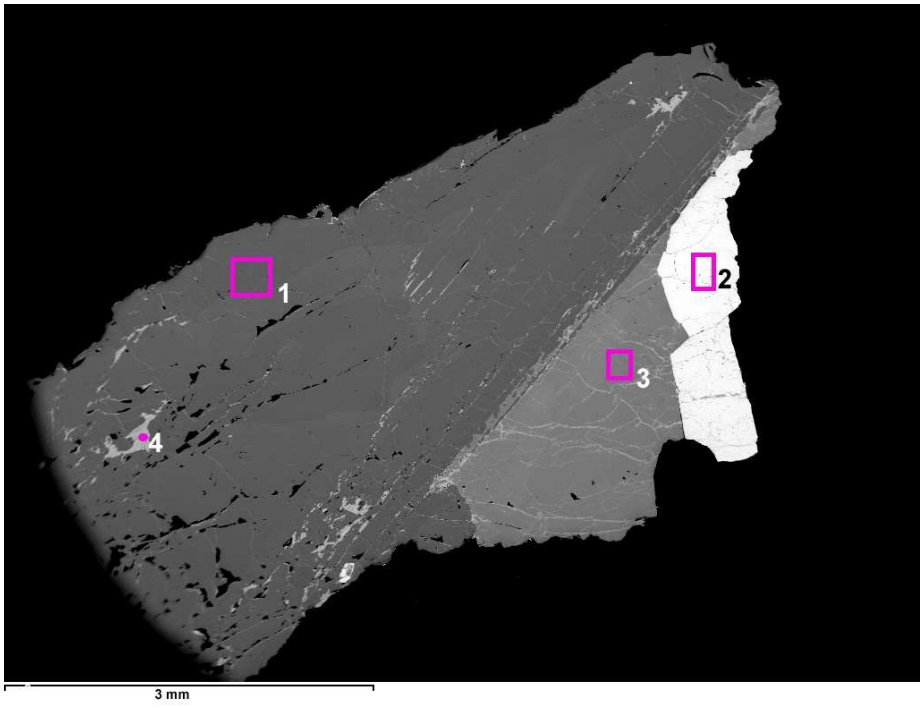

501

Figure 3 TL glow curves of *Ale I* (a) and *Ale II* (b) samples of natural alexandrite, using a 5˚C/s heating rate. The inset shows intensity of the high temperature peak for each curve as a function of dose.

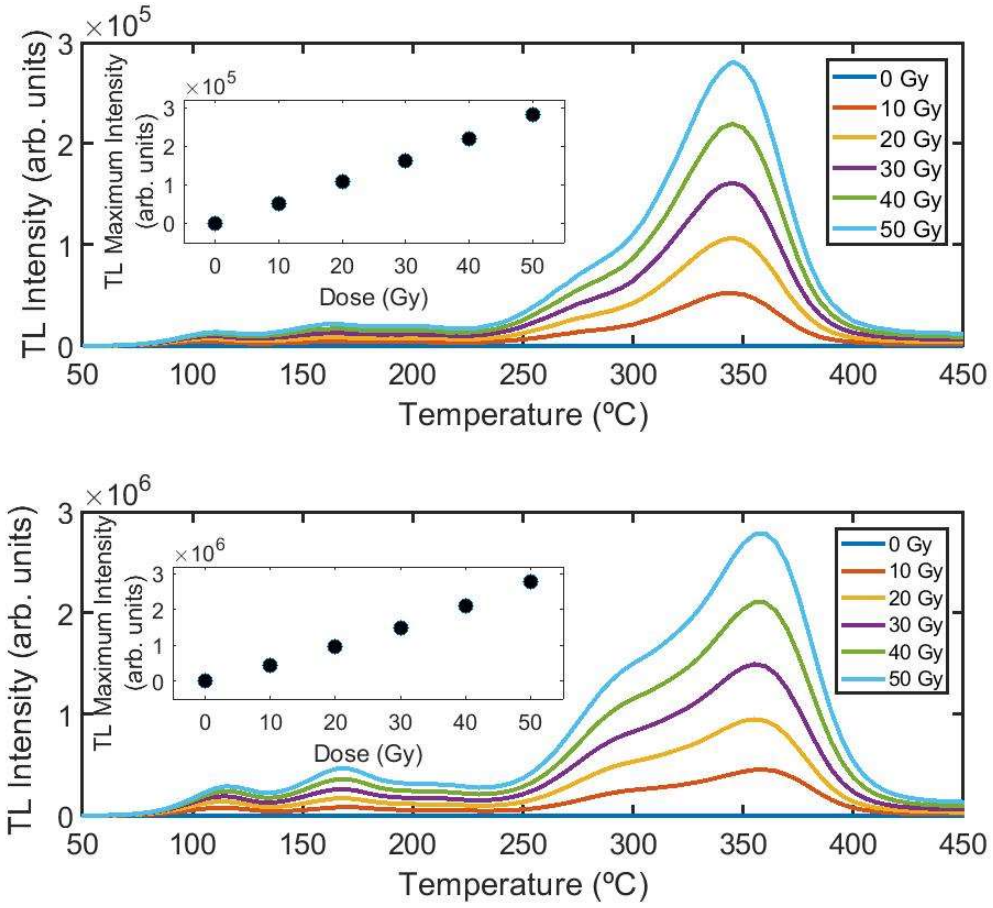

Figure 4 Linear regression from the TL normalized intensity of the high temperature peak as a function of the dose for *Ale I* (a) and *Ale II* (b) samples.

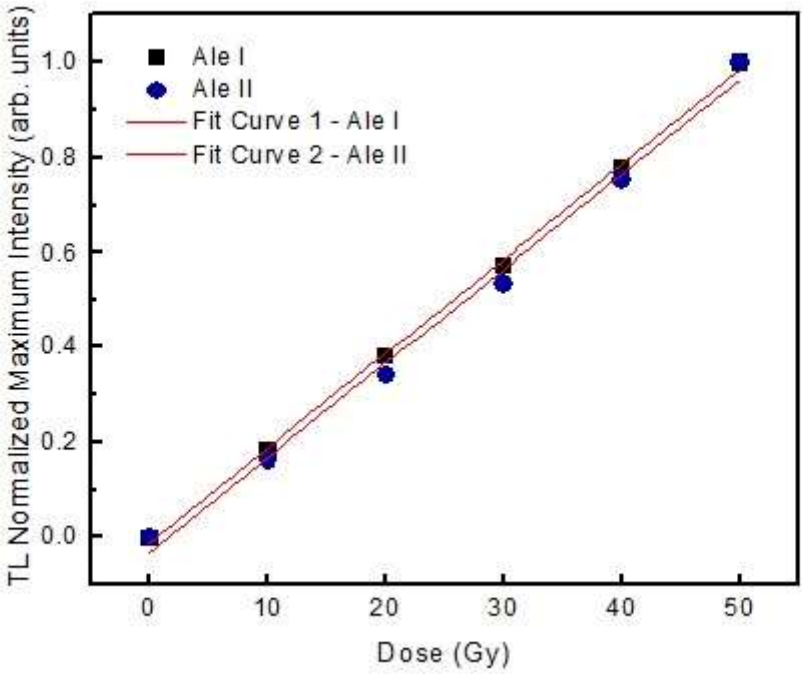

Figure 5 TL glow curves of *Ale I* (a) and *Ale II* (b) samples of natural alexandrite, using 5˚C/s heating rate and dose 1Gy. The inset shows intensity of the high temperature peak for each curve as a function of pause time.

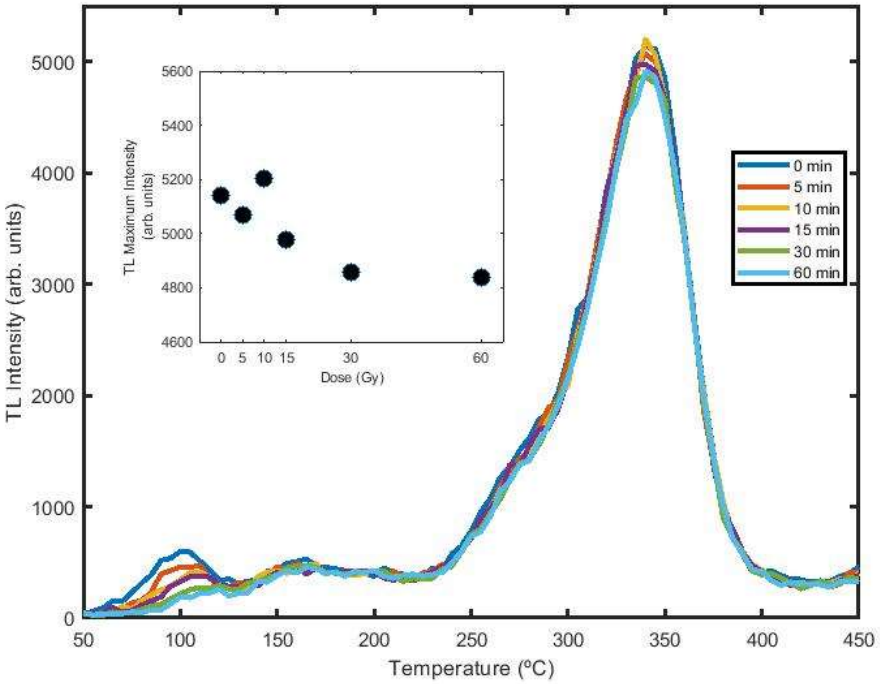

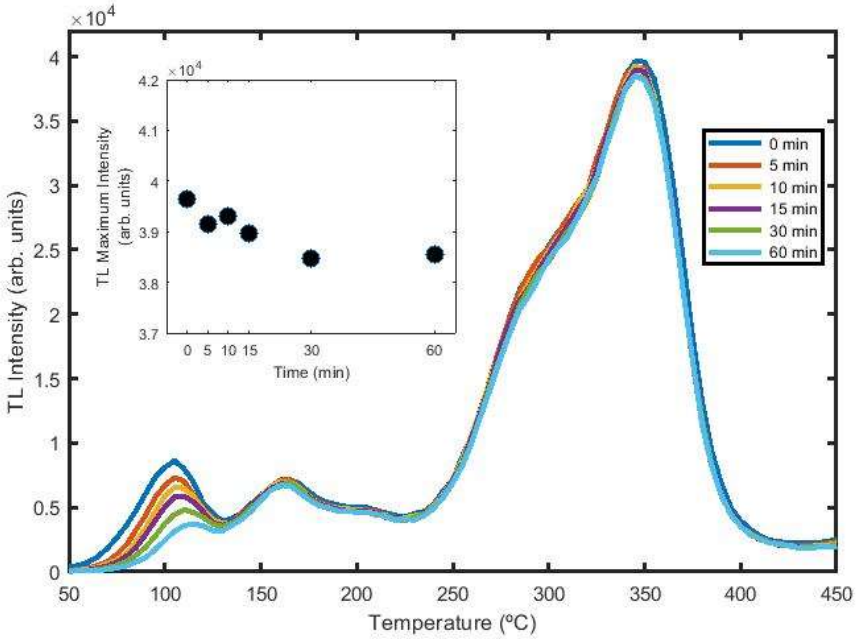

TABLE CAPTIONS

Table 1 X-ray fluorescence bulk analysis results of *Ale I* and *Ale II* samples of natural alexandrite. All results in wt%; normalized results.

Sample	MgO	Al_2O_3	SiO_2	P_2O_5	CaO	TiO_2	Cr_2O_3	Fe_2O_3
Ale I	0.495	96	<0.001	<0.001	<0.001	0.391	0.89	2.2
Ale II	2.66	76.6	8.29	4.42	3.52	<0.001	1.29	3.24

Table 2 EDS results of sample *Ale I* at different regions. All results in wt%; non-normalized results; Al – alexandrite; M - phlogopite-biotite.

Phase	Area/point	MgO	Al_2O_3	SiO_2	K_2O	TiO_2	Cr_2O_3	MnO	Fe_2O_3	Total
Al	1	-	77.25	-	-		0.31	-	1.62	79.18
Al	2	-	76.89	-	-	0.32	0.43	-	1.26	78.90
Al	3	-	75.62	-	-	0.19	0.42	-	1.47	77.70
Al	4	-	71.67	-	-	0.16	0.96	-	1.23	74.01
M	5	19.21	18.51	31.87	4.01	-	0.76	0.49	12.79	87.65
M	6	22.29	21.46	27.89	-	-	0.55	0.43	15.52	88.14
M	7	18.15	20.77	24.98	-	-	0.87	0.49	18.02	83.28
M	8	19.36	22.44	26.87	-	-	0.86	0.85	18.85	89.22

576 **Table 3** EDS results for sample *Ale II* at different regions. All results in wt%. Al –
577 alexandrite; Ap – apatite; M - phlogopite-biotite.

Phase	Area/point	MgO	Al_2O_3	SiO_2	P_2O_5	CaO	Cr_2O_3	MnO	Fe_2O_3	Total
Al	1	-	78.75	0.29	-	-	0.51	-	1.83	81.38
Ap	2	0.37	0.36	-	41.05	50.61	-	0.23	0.22	92.84
M	3	9.95	27.69	33.62	-	2.38	0.24	-	4.12	79.47
M	4	23.93	24.01	29.85	-	-	0.37	0.55	18.1	96.83

578
579
580
581
582
583
584
585
586
587
588
589
590
591
592
593
594
595
596
597
598
599

600 **Table 4** Parameters determined in a linear fit (y = a + b * x) from the normalized peak
601 maximum intensity of the high temperature TL peak for *Ale I* and *Ale II* samples.

Fit Parameters		
Sample	a (a.u.)	b (a.u./Gy)
Ale I	-0.012 (±0.009)	0.01995 (±0.00029)
Ale II	-0.032 (±0.023)	0.01992 (±0.00074)

602

603